ISSN 0023-1584, Kinetics and Catalysis, 2009, Vol. 50, No. 2, pp. 241–246. © Pleiades Publishing, Ltd., 2009.
Original Russian Text © D.V. Andreev, S.V. Korotaev, R.M. Khantakov, L.L. Makarshin, A.G. Gribovskii, L.P. Davydova, V.N. Parmon, 2009, published in Kinetika i Kataliz, 2009, Vol. 50, No. 2, pp. 256–261.

Effect of the Cerium Content on the Activity of Cu–Ce–Al–O Catalysts in the Methanol Steam Reforming Reaction in a Flow Reactor

D. V. Andreev, S. V. Korotaev, R. M. Khantakov, L. L. Makarshin, A. G. Gribovskii, L. P. Davydova, and V. N. Parmon

Boreskov Institute of Catalysis, Siberian Branch, Russian Academy of Sciences, Novosibirsk, 630090 Russia
e-mail: andreev@catalysis.ru

Received December 14, 2007

Abstract—The $Cu_{18.5}Ce_xAl_{81.5-x}$ (where x = 2, 7.4, and 14) oxide catalysts were synthesized by coprecipitation and tested in the methanol steam reforming reaction in an integral flow reactor at 270°C. It was found that the activity of the catalysts increased with the calcination temperature and catalysts with intermediate cerium contents exhibited the highest activity; these catalysts exhibited the greatest values of S_{BET} and S_{Cu}. The phase analysis demonstrated that copper in these samples occurred almost entirely as a $CuO–CeO_2$ solid solution. The concentration of carbon monoxide at the reactor outlet decreased with the calcination temperature. For the most active sample with a cerium content of 7.4% calcinated at 700°C, the concentration of CO reached a minimum of no higher than 0.3%.

DOI: 10.1134/S0023158409020141

INTRODUCTION

Catalytic processes are most promising for the manufacture of hydrogen-containing fuels in compact devices like fuel processors. In this context, the development of highly efficient specialized catalysts for corresponding devices is a problem of paramount importance.

The production of hydrogen in fuel processors with the use of the endothermic reaction of methanol steam reforming is of intense interest:

$$CH_3OH + H_2O \longrightarrow CO_2 + 3H_2 \quad (\Delta_r H^\circ_{298} = 49\ \text{kJ/mol}), \quad \text{(I)}$$

$$CO_2 + H_2 \longrightarrow CO + H_2O \quad (\Delta_r H^\circ_{298} = 41\ \text{kJ/mol}). \quad \text{(II)}$$

Reaction (II)—the reversed water gas shift reaction—leads to the formation of CO, which is an extremely undesirable product for low-temperature fuel cells [1]. The reaction of methanol steam reforming is usually performed on various copper-containing catalysts, such as Cu/ZnO [2], $Cu/ZnO/Al_2O_3$ [3], and Cu/Al_2O_3 [4], as well as on palladium-containing catalysts like Pd/ZnO [5, 6].

It is well known that the activity and stability of copper-containing catalysts considerably increases after the introduction of promoting additives. Thus, according to published data [4, 7], after the addition of manganese to the Cu/Al_2O_3 catalyst, its activity increased because of the formation of active centers like Cu^0–Mn_2O_3, at which the dissociation of methanol and water occurred. The partial or full replacement of Al by Zr in the Cu/Al_2O_3 catalysts resulted in the formation of Cu_2O crystallites in the course of the reaction. These crystallites prevented catalyst deactivation and, unlike Cu^0, active component agglomeration [8].

Recently, attention has been focused on the modification of copper–alumina catalysts with cerium. This is due to the high mobility of oxygen in the lattice of cerium dioxide and the capacity of this oxide used as a support for strong interaction with active component cations. Cerium(IV) oxide has a fluorite-type cubic lattice and forms substitutional solid solutions with various cations, in particular, Cu^{2+}. This results in the modification of the structural properties of the active component—copper. There is evidence that cerium dioxide is not only a structural promoter but also it plays a key role in the water gas shift reaction [9] to decrease the concentration of CO at the reactor outlet and thus to facilitate the subsequent removal of CO by selective oxidation [10]. The promotion of Cu/Al_2O_3 with the use of Zr and Ce increased the activity of the catalysts in methanol steam reforming in the order Cu–Al < Cu–Zn–Al < Cu–Zn–Ce–Al [11]. According to Patel and Pant [11], the degree of dispersion of copper metal in the catalyst decreased after the addition of Ce; thereby, the catalyst activity was increased. The occurrence of mobile oxygen in cerium dioxide also inhibited the deactivation of cerium-modified catalysts to facilitate the conversion of coke into carbon oxides. According to Mastalir et al. [12], the presence of ZrO_2 and CeO_2

Table 1. Compositions and calcination temperatures of the synthesized catalysts

Symbol	Catalyst composition, at %	Calcination temperature, °C
C2-100	Cu18.5–Ce2–Al79.5	100 (drying)
C7.4-100	Cu18.5–Ce7.4–Al74.1	100 (drying)
C14-100	Cu18.5–Ce14–Al67.5	100 (drying)
C2-400	Cu18.5–Ce2–Al79.5	400
C2-550	Cu18.5–Ce2–Al79.5	550
C2-700	Cu18.5–Ce2–Al79.5	700
C7.4-400	Cu18.5–Ce7.4–Al74.1	400
C7.4-550	Cu18.5–Ce7.4–Al74.1	550
C7.4-700	Cu18.5–Ce7.4–Al74.1	700
C14-400	Cu18.5–Ce14–Al67.5	400
C14-550	Cu18.5–Ce14–Al67.5	550
C14-700	Cu18.5–Ce14–Al67.5	700

among the constituents of copper catalysts facilitated the reduction of copper in the course of the reaction.

In this work, we studied the effect of the cerium content and synthesis temperature of Cu–Ce–Al–O catalysts at a constant copper content on the activity of the catalysts in methanol steam reforming in a plug-flow reactor, which simulated the operation of a microreactor for hydrogen generation.

EXPERIMENTAL

Catalyst Synthesis

The $Cu_{18.5}Ce_xAl_{81.5-x}$ catalysts with $x = 2$, 7.4, and 14 were prepared by coprecipitation with the use of sodium carbonate. For this purpose, 1 M solutions of cerium nitrate ($Ce(NO_3)_2 \cdot 6H_2O$, chemically pure), copper nitrate ($Cu(NO_3)_2 \cdot 3H_2O$, chemically pure), and aluminum nitrate ($Al(NO_3)_2 \cdot 9H_2O$, chemically pure) were mixed in the required ratios and heated to 60°C. A solution of sodium carbonate (1 M) was slowly added to the solution of metal nitrates with intense stirring to obtain pH 8–9. Then, the resulting precipitate was aged (1 h), filtered off, washed several times with warm distilled water to remove Na^+ cations, and dried at 100°C for 12 h. To obtain the final product, i.e., the catalyst, the dry mixture was calcinated at various temperatures (from 400 to 700°C) for 4 h. Table 1 summarizes data on the compositions of the synthesized catalysts and final calcination temperatures.

Catalyst Characterization

X-ray diffraction (XRD). The samples of Cu–Ce–Al–O catalysts before and after calcination were studied on a Siemens X-ray diffractometer (Germany) (CuK_α radiation with a graphite monochromator on a reflected beam) over the angle range $2\theta = 20°–70°$. The phase composition was identified using the JCPDS files (PC PDF Win 2000). The following structures were taken as the theoretical basis for the samples: the cubic structure of CeO_2 [JCPDS, 43-1002; $a = 5.411$ Å], the cubic structure of $CuAl_2O_4$ [JCPDS, 33-0448; $a = 8.075$ Å], and the monoclinic structure of CuO [JCPDS, 05-0661; $a = 4.684$ Å, $b = 3.425$ Å, $c = 5.129$ Å, and $\beta = 99.47°$].

Specific surface area measurements. The specific surface areas (S_{BET}) of the samples were measured by the BET method on an ASAP-2400 automated instrument using nitrogen adsorption isotherms at 77 K (the cross section of the nitrogen molecule was taken to be 16.2 $Å^2$).

To determine the specific surface area of copper metal in the catalysts, titration based on the oxidation reaction of surface copper atoms with nitrous oxide, $2Cu_s + N_2O_{gas} \longrightarrow Cu_2O_s + N_{2,\,gas}$, was used. The initial catalyst (0.5–1 g) with a particle size of 0.25–0.5 mm was loaded in a 3-cm^3 reactor, which was placed in a fast-response furnace. Then, the sample was activated in a flow of hydrogen with increasing temperature from 150 to 270°C at a rate of 60 K/h. Thereafter, the reduced catalyst was cooled to room temperature. The specific surface areas of copper were determined by chromatographic analysis from the concentrations of nitrogen after the pulse supply of N_2O into the reactor.

Determination of the Activity of Catalysts in Methanol Steam Reforming

The schematic diagram of the setup and the procedure used for the measurement of catalyst activity in methanol steam reforming were described elsewhere [13]. The fixed-bed reactor was a stainless steel tube with an inner diameter of 3 mm and 40 cm in length equipped with an evaporator for the water–methanol mixture. The reactor was placed in a tube furnace, whose temperature was regulated and maintained to within 1 K with the use of an RIF-101 automatic temperature regulator. The catalyst particle size was 0.25–0.5 mm, and the catalyst weight was 0.25 g. A mixture of methanol and water (1 : 1, mol/mol) was dispensed and supplied to the reactor with the use of a Bi-flow system (Boreskov Institute of Catalysis, Siberian Branch, Russian Academy of Sciences). The gas flow from the reactor passed through a condensate collector and arrived at the LKhM-8 chromatograph (column, 3 m; solid support, Sibunit; column temperature, room temperature). The outlet flow rate was measured with a foam flow meter. Before the beginning of the experiment, the catalyst was activated in a flow of the starting water–methanol mixture at 270°C for 2 h. The reaction of methanol steam reforming was performed at 270°C. This temperature was chosen based on the data of preliminary experiments, which demonstrated that the concentration of CO (which is a catalytic poison for low-temperature fuel cells) at the reactor outlet dramat-

ically increased at higher temperatures, whereas the activity of the catalysts decreased at $T < 270$°C.

The initial experimental data were the dependences of methanol conversion on the reduced contact time W/F, where W is the catalyst weight (g) and F is the flow of methanol at the reactor inlet (mmol/min). The main reaction products are H_2, CO_2, and CO (<1 mol %). According to mass-spectrometric data, other possible by-products of the methanol steam reforming process (formaldehyde, formic acid, dimethyl ether, and methyl formate) were not detected.

RESULTS

Phase Composition of the Catalysts

Figure 1 shows the X-ray diffraction patterns of catalyst samples with various cerium contents. It can be seen that uncalcinated samples were X-ray amorphous: reflections from copper-containing phases were absent; however, peaks due to the CeO_2 phase appeared as the cerium content was increased. The calcination of the samples did not result in the appearance of peaks due to Al_2O_3; this is indicative of the absence of individual crystalline alumina phases. As the calcination temperature was increased, more pronounced reflections from the CeO_2 phase and reflections from new crystalline phases (CuO and the copper–aluminum spinel $CuAl_2O_4$) appeared. In this case, the fraction of the CuO phase decreased with cerium concentration. Moreover, the peak of the spinel phase reached a minimum in the sample containing 7.4 at % cerium. The low intensity of copper oxide peaks is explained by the fact that CuO can form several species: (a) a solid solution with cerium dioxide (CuO–CeO_2) and (b) the copper–aluminum spinel $CuAl_2O_4$. In addition, small copper oxide crystallites can be dispersed on the surface of aluminum oxide, and they cannot be identified using XRD analysis because of their small size. It is likely that all of the above situations occurred in the case under consideration, and the change in the phase composition was nonmonotonic.

Specific Surface Areas of the Catalysts

As expected, an increase in the calcination temperature (T_{calc}) from 400 to 700°C resulted in a decrease in S_{BET} by a factor of 1.4–1.6; this was due to an increase in the crystallite sizes of the cerium dioxide and copper–aluminum spinel phases (Table 2). In this case, the total pore volume decreased and the average pore diameter increased. The highest degree of dispersion was observed in the samples containing an intermediate cerium concentration of 7.4 at %. However, these samples exhibited the greatest average pore size. It is believed that C7.4 catalysts had a more extended and branched pore structure than that of other samples.

The results of the measurements of the specific surface area of copper metal demonstrated that the specific surface area of copper metal (S_{Cu}) increased with the T_{calc} of catalysts, and the C7.4-700 sample exhibited a maximum degree of dispersion of copper among the samples with various cerium contents.

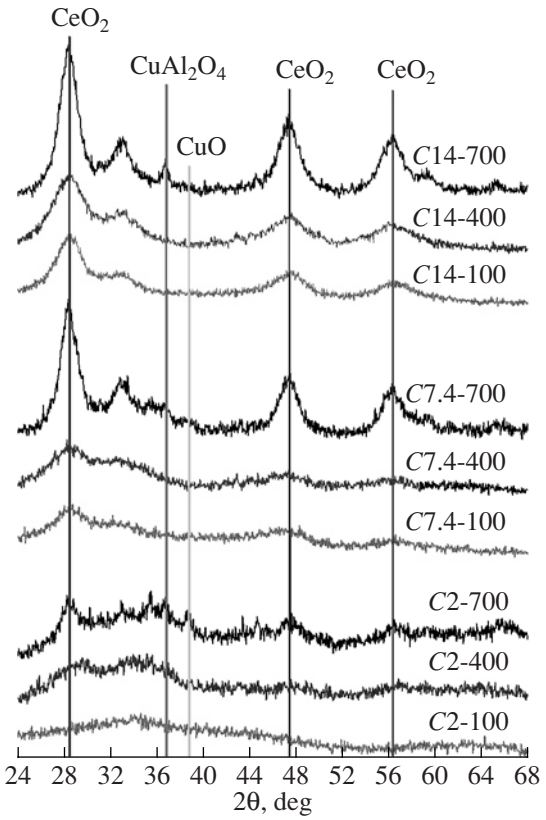

Fig. 1. XRD patterns from the catalysts. See Table 1 for notation.

Activity of the Catalysts

Figure 2 shows the dependence of methanol conversion on the value of W/F for catalysts with various

Table 2. Texture characteristics of the catalysts

Sample	S_{BET}, m^2/g	Total pore volume, cm^3/g	Average pore size, nm	S_{Cu}, m^2/g
C2-400	175	0.348	7.93	–
C7.4-400	207	0.470	9.08	2.7
C14-400	159	0.296	7.45	–
C2-550	175	0.360	8.22	–
C7.4-550	181	0.439	9.69	7.0
C14-550	172	0.368	8.55	–
C2-700	113	0.326	11.5	3.9
C7.4-700	128	0.310	10.2	10.5
C14-700	113	0.235	8.33	1.9

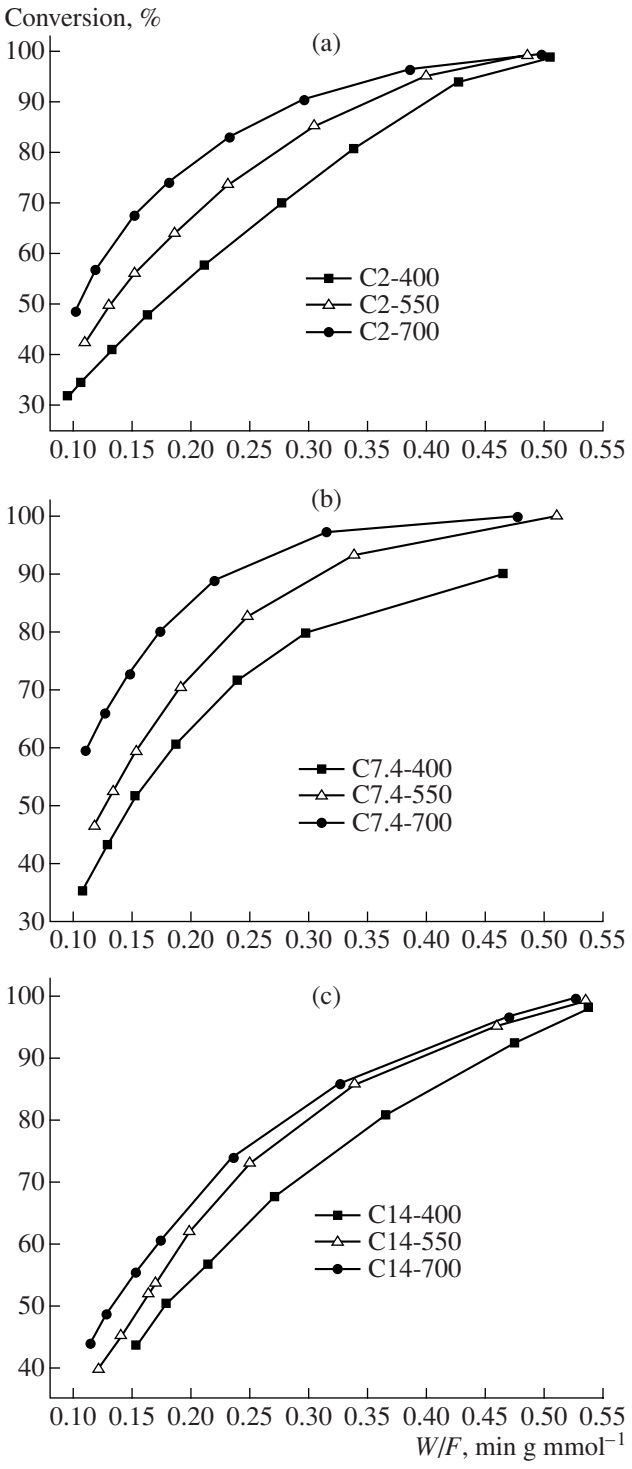

Fig. 2. Dependence of methanol conversion on *W*/*F* for samples containing (a) 2, (b) 7.4, and (c) 14 at % Ce.

cerium contents calcinated at various temperatures. Because it is impossible to measure the true activity of a catalyst in a plug-flow reactor, the capacity of a catalyst for hydrogen at 80% methanol conversion was taken as a criterion for catalyst activity. Table 3 summarizes the results of the measurements of the capacity for hydrogen and the level of CO at the reactor outlet for the catalysts at 270°C.

Control experiments on the activation of catalysts in a flow of hydrogen (10 vol % H_2 in Ar) at 220°C for 1 h before the onset of the methanol steam reforming reaction demonstrated an increase in the activity of samples calcinated at 700°C. Regardless of the Ce content of the catalysts, the capacity for hydrogen was 18.4 l g_{Cat}^{-1} h^{-1}, which is comparable with the best C7.4-700 sample, which was preactivated with the initial water–methanol mixture.

From data in Table 3, it follows that the yield of hydrogen increased with T_{calc}. The samples containing 7.4% Ce exhibited a higher activity. Note that, in addition, an increase in T_{calc} resulted in a decrease in the concentration of CO at the reactor outlet. An increase in the cerium content from 2 to 7.4 at % for each series of catalysts calcinated at various temperatures also resulted in a decrease in the concentration of CO. The lowest yield of carbon monoxide was observed on the C7.4-700 catalyst calcinated at 700°C. Note that, for all of the catalyst compositions, the level of CO at the reactor outlet at 270°C was much lower than the equilibrium thermodynamic value calculated for methanol steam reforming reaction conditions. It is believed that this is due to a decrease in the rate of reaction (II). At the same time, the activity of the catalysts correlated with the value of S_{Cu}. Thus, catalyst calcination at 700°C caused an increase in S_{Cu} and, as a result, an increase in the catalyst activity. The best results were obtained in the C7.4-700 sample with S_{Cu} of 10.5 m^2/g, which is greater than that of the other samples by a factor of 2–3.

DISCUSSION

The following conclusions can be made based on a comparison between the experimental data on the activity of the synthesized catalysts in the methanol steam reforming reaction and the structure characteristics of these catalysts.

The samples with a cerium concentration of 7.4 at % exhibited maximum activity. The results of the BET measurements of specific surface areas (Table 2) demonstrate that S_{BET} for catalysts from each particular series calcinated at 400, 550, and 700°C reached a maximum in samples with an intermediate concentration of cerium. The measurement of S_{Cu} also demonstrated that the surface area of copper particles reached a maximum in the sample containing 7.4 at % Ce. This fact suggests a correlation between the accessible surface area of the active component and the efficiency of catalyst operation.

It was found that the addition of CeO_2 to the copper–alumina system affected the degree of dispersion of the active component. According to XRD data, in the catalysts with a maximum cerium content calcinated at 700°C, copper occurred in the following three phases:

copper–aluminum spinel ($CuAl_2O_4$), solid solution with cerium dioxide ($CuO–CeO_2$), and copper oxide (CuO).

It is believed that the main portion of copper occurred as CuO and $CuAl_2O_4$ at a minimum cerium content. At the same time, copper almost entirely occurred in the $CuO–CeO_2$ solid solution in the samples with an intermediate composition in terms of cerium. It is likely that, in addition to data published by Liu et al. [14], who demonstrated a limited solubility of CuO in CeO_2, we observed another situation—a limited solubility of CeO_2 in CuO at a high cerium content of the catalyst. The formation of a $CeO_2–CuO$ solid solution was supported by the change in the lattice parameter of cerium dioxide: the tabulated value of parameter *a* for the cubic structure of CeO_2 (5.411 Å) decreased to 5.405–5.408 Å. This was due to the much smaller size of the Cu^{2+} cation, 0.79 Å against 0.92 Å for the Ce^{4+} cation [15]. The pattern of the insertion of copper into the lattice of cerium dioxide can be more complicated: according to Fernándes-Garcia et al. [16], only a part of CuO can form a solid solution with CeO_2 to afford $Ce_{0.8}Ce_{0.2}O_x$; the other copper oxide occurs as small crystallites on the surface of the resulting solid solution.

According to published data [17, 18], the nature of the copper-containing phase strongly affects its capacity to reduction and, consequently, its activity in methanol steam reforming. Copper is most active as a constituent of a solid solution of CuO in CeO_2, which stabilizes the small crystallites of copper metal in the course of reaction to prevent them from agglomeration. We observed this behavior in the most active C7.4-700 sample, where copper almost entirely occurs as a solid solution. As for the samples calcinated at lower temperatures (400 and 550°C), the XRD spectra suggest that these catalysts are X-ray amorphous; this is likely due to an insufficient regularity of the solid solution of CuO in CeO_2.

Based on the reaction mechanism of methanol steam reforming proposed by Men et al. [18], we assume that the following two conditions should be simultaneously satisfied for the high activity of copper–cerium catalysts: (a) the solid solution of copper and cerium oxides should be crystalline rather than amorphous and (b) a certain ratio between the concentrations of copper and cerium cations should take place in this solid solution. It is believed that the active centers of the catalyst are arranged at the interface between copper metal reduced in the course of methanol steam reforming and CeO_2, which is a source of mobile oxygen, which migrates to Cu^0. Therefore, the regular crystal structure of a solid solution makes it possible to form a sufficient amount of interfaces in the course of the reaction. At a high Ce/Cu ratio, coarse CeO_2 crystallites are formed, and these crystallites can block a part of the surface of active copper, whereas large Cu^0 crystallites with a smaller specific surface area are formed at a low Ce/Cu ratio. It is likely that, at an optimum ratio between the crystallite sizes of cerium dioxide and copper metal, which corresponds to an intermediate concentration of cerium, the accessibility of the active copper component in the course of methanol steam reforming reached a maximum.

Table 3. Results of the measurements of the activity of $Cu_{18.5}Ce_xAl_{81.5-x}O$ catalysts in the methanol steam reforming reaction at 270°C

Catalyst	H_2 capacity*, l g_{Cat}^{-1} h^{-1}	Outlet concentration of CO,* %
C2-400	10.5	0.60
C2-550	12.9	0.51
C2-700	16.3	0.45
C7.4-400	11.7	0.59
C7.4-550	15.0	0.44
C7.4-700	20.2	0.32
C14-400	9.7	0.46
C14-550	11.6	0.45
C14-700	12.5	0.36

* At 80% methanol conversion.

The experimental results showed that copper as the constituent of a solid solution was most active in the methanol steam reforming reaction. Indeed, if copper is the active component and the copper contents of all of the samples are the same, the activity of these samples will be the same. However, catalysts with minimum and maximum cerium concentrations exhibited a reduced activity. Consequently, taking into account the results of structural measurements in the catalysts, we can conclude that, at a certain concentration of Ce, copper can occur as a constituent of spinel or CuO, which are less active than the solid solution containing a maximum amount of copper at a cerium concentration of 7.4 at %. However, the use of a stronger reducing agent—a mixture of 10% hydrogen in argon—makes it possible to activate all the copper. In this case, the activity of the C2-700 and C14-700 samples increases to reach the activity of the C7.4-700 sample (Table 3).

Copper-containing catalysts are also highly active in the water gas shift reaction [19–22]. From the experimental results, it follows that the active sites of copper as a constituent of a $CuO–CeO_2$ solid solution are active toward both of the reactions. According to published data [23, 24], the decreased experimental values of CO concentrations in a mixture at the reactor outlet suggest that CO is a secondary product, which is not formed by the decomposition of methanol into hydrogen and CO. The behavior observed can be explained if reaction (II) is kinetically suppressed, and it does not reach equilibrium [25].

ACKNOWLEDGMENTS

This work was performed within the framework of a state contract with the Federal Agency for Science and Innovations (contract no. EE-13.2/002) and supported by the Council of the President of the Russian Federation for Support of Young Scientists and Leading Scientific Schools (grant no. NSh-6536.2006.3; state contract no. 02.445.11.7282).

REFERENCES

1. *Fuel Cell Handbook*, Morgantown, W.Va.: US Department of Energy, Office of Fossil Energy, National Energy Technology Laboratory, 2000, 5th ed.
2. Agrell, J., Boutonnet, M., Melian-Cabrera, I., and Fierro, J.L.G., *Appl. Catal., A*, 2003, vol. 253, no. 1, p. 201.
3. Shen, J.P. and Song, C., *Catal. Today*, 2002, vol. 77, nos. 1–2, p. 89.
4. Idem, R.O. and Bakhshi, N.N., *Ind. Eng. Chem. Res.*, 1994, vol. 33, no. 9, p. 2056.
5. Chin, Y.H., Dagle, R., Hu, J., Dohnalkova, A.C., and Wang, Y., *Catal. Today*, 2002, vol. 77, nos. 1–2, p. 79.
6. Cao, C., Xia, G., Holladay, J., Jones, E., and Wang, Y., *Appl. Catal., A*, 2004, vol. 262, no. 1, p. 19.
7. Idem, R.O. and Bakhshi, N.N., *Chem. Eng. Sci.*, 1996, vol. 51, no. 14, p. 3697.
8. Ritzkopf, I., Vukojevic, S., Weidenthaler, C., Grunwaldt, J.-D., and Schuth, F., *Appl. Catal., A*, 2006, vol. 302, no. 2, p. 215.
9. Li, Y., Fu, Q., and Flytzani-Stephanopoulos, M., *Appl. Catal., B*, 2000, vol. 27, no. 3, p. 179.
10. Wang, S.-P., Wang, X.-Y., Huang, J., Zhang, S.-M., Wang, S.-R., and Wu, S.-H., *Catal. Commun.*, 2007, vol. 8, no. 3, p. 231.
11. Patel, S. and Pant, K.K., *J. Power Sources*, 2006, vol. 159, no. 1, p. 139.
12. Mastalir, A., Frank, B., Szizybalski, A., Soerijanto, H., Deshpande, A., Niederberger, M., Schomacker, R., Schlogl, R., and Ressler, T., *J. Catal.*, 2005, vol. 230, no. 2, p. 464.
13. Makarshin, L.L., Andreev, D.V., Gribovskiy, A.G., and Parmon, V.N., *Int. J. Hydrogen Energy*, 2007, vol. 32, no. 16, p. 3864.
14. Liu, Y., Hayakawa, T., Suzuki, K., Hamakawa, S., Tsunoda, T., Ishii, T., and Kumagai, M., *Appl. Catal., A*, 2002, vol. 223, nos. 1–2, p. 137.
15. *Lang's Handbook of Chemistry*, Dean, J.A., Ed., New York: McGraw-Hill, 1985, p. 3.
16. Fernández-Garcia, M., Gómez Rebollo, E., Guerrero Ruiz, A., Conesa, J.C., and Soria, J., *J. Catal.*, 1997, vol. 172, no. 1, p. 146.
17. Zhang, X. and Shi, P., *J. Mol. Catal. A: Chem.*, 2003, vol. 194, nos. 1–2, p. 99.
18. Men, Y., Gnaser, H., Zapf, R., Hessel, V., Ziegler, C., and Kolb, G., *Appl. Catal., A*, 2004, vol. 277, nos. 1–2, p. 83.
19. Baronskaya, N.A., Yurieva, T.M., Minyukova, T.P., Demeshkina, M.P., Khassin, A.A., and Sipatrov, A.G., *Catal. Today*, 2005, vol. 105, nos. 3–4, p. 697.
20. Agrell, J., Birgersson, H., and Boutonnet, M., *J. Power Sources*, 2002, vol. 106, nos. 1–2, p. 249.
21. Geissler, K., Newson, E., Vogel, F., Truong, T.-B., Hottinger, P., and Wokaun, A., *Phys. Chem. Chem. Phys.*, 2001, vol. 3, p. 289.
22. Purnama, H., Ressler, T., Jentoft, R.E., Soerijanto, H., Schlogl, R., and Schomacker, R., *Appl. Catal., A*, 2004, vol. 259, no. 1, p. 83.
23. Peppley, B.A., Amphett, J.C., Kearns, L.M., and Mann, R.F., *Appl. Catal., A*, 1999, vol. 179, nos. 1–2, p. 31.
24. Lee, J.K., Ko, J.B., and Kim, D.H., *Appl. Catal., A*, 2004, vol. 278, no. 1, p. 25.
25. Galvita, V., Semin, G.L., Belyaev, V.D., Yurieva, T.M., and Sobyanin, V.A., *Appl. Catal., A*, 2001, vol. 216, nos. 1–2, p. 85.